

Preparation and magnetic properties of the $(1-x)\text{BiFeO}_3 - x\text{BaTiO}_3$ solid solutions

A. IANCULESU^a, L. MITOSERIU^{b*}, H. CHIRIAC^c, M.M. CARNASCIALI^d, A. BRAILEANU^e, R. TRUSCA^f

^a*Polytechnics University of Bucharest, 1-7 Gh. Polizu, P.O. Box 12-134, 011061 Bucharest, Romania*

^b*Department of Solid State and Theoretical Physics, Al. I. Cuza Univ., 11 Bv. Carol I, 700506 Iasi, Romania*

^c*National Institute of Research and Development for Technical Physics, Iasi 700050, Romania*

^d*Dept. of Chemistry and Industrial Chemistry, Univ. of Genoa, 31 Via Dodecaneso, Genoa I-16146, Italy*

^e*Institute of Physical Chemistry Ilie Murgulescu of the Romanian Academy, 202 Spl. Independentei, 060021 Bucharest, Romania*

^f*S.C. METAV – Research & Development Bucharest, 31 C. A. Rosetti, 020011 Bucharest, Romania*

$(1-x)\text{BiFeO}_3 - x\text{BaTiO}_3$ ($0 \leq x \leq 0.30$) ceramics were prepared by the solid state reaction method. After sintering at $800^\circ\text{C}/1\text{h}$ and slow cooling, single phase compositions were obtained for both presintered and sintered samples, including the composition $x=0$, which was rarely reported. The gradual attenuation of the rhombohedral distortion with the increase of BaTiO_3 content was pointed out. The BaTiO_3 admixture acts also as inhibitor for the grain growth process, contributing to the decrease of the average grain size. The compositions corresponding to $x=0.30$ exhibits multiferroic behavior at room temperature, having both antiferromagnetic and ferroelectric order and low losses (< 3%). The Raman activity proved the existence of the local non-centrosymmetry and of some grain boundary characteristics at room temperature. The magnetic data indicates a composition-dependent antiferromagnetic character.

(Received April 1, 2008; accepted June 30, 2008)

Keywords: Magnetic properties, Solid solutions BiFeO_3 - BaTiO_3

1. Introduction

BiFeO_3 , one of the very few known multiferroic compounds, showing ferroelectric and antiferromagnetic order, recently attracted a high interest and controversial discussions [1 - 3]. At room temperature BiFeO_3 presents a rhombohedrally-distorted perovskite structure of $R3c$ type ($a = b = c = 3.96 \text{ \AA}$, $\alpha = \beta = \gamma = 89.4^\circ$). Although at the beginning BiFeO_3 was considered an antiferroelectric because of its superstructure and of the low value of the dielectric constant, recently it was classified as ferroelectric and ferroelastic, with a Curie temperature T_C around 830°C . BiFeO_3 is also an antiferromagnet, with a Néel temperature T_N of $\sim 310^\circ\text{C}$ [4, 5], exhibiting a weak ferro-ferrimagnetic characteristic in some temperature ranges [6]. Due to the high Curie temperature, it was expected that BiFeO_3 presents a high spontaneous polarization in its ferroelectric state. Contrarily to this assumption, experimental data revealed low values of both spontaneous polarization and dielectric permittivity at room temperature, mainly because of the semiconducting nature of BiFeO_3 , involving high values of dielectric losses. The conduction phenomena in BiFeO_3 are complex, taking into account that beside the polaronic mechanism, an ionic conductivity due to the formation of oxygen vacancies as compensating defects for the partial reduction of Fe^{3+} to Fe^{2+} could not be excluded. The low

resistivity hinders the ferroelectric hysteresis, limiting therefore the application of this compound. Another problem of BiFeO_3 consists in the difficulty of its obtaining as single-phase material in its ceramic form. Usually, small amounts of bismuth-rich secondary phase with controversial composition, corresponding either to $\text{Bi}_{40}\text{Fe}_{2}\text{O}_{63}$ (according to the phase diagram [7]) or to $\text{Bi}_{36}\text{Fe}_{2}\text{O}_{57}$ (according to JCPDS no. 42-0181), are detected in the X-ray diffraction pattern of these ceramics. This segregation of the residual phases at the grain boundary could also play a role in the change of dielectric behaviour, resulting in the rise of electrical conductivity and leakage current, especially at higher temperatures.

In order to avoid all these disadvantages, i.e. to stabilize a single-phase composition and to improve the ferroelectric behaviour, the obtaining of some binary solid solutions with other perovskite compounds with better dielectric and ferroelectric characteristics, as BaTiO_3 [2, 8, 9] or PbTiO_3 [10] seems to be a suitable approach. Taking into account the actual trend to eliminate the lead compounds from the industrial application, our attention was focused on the investigation of the phase composition, microstructure and electrical characteristics of some $\text{Bi}_{1-x}\text{Ba}_x\text{Fe}_{1-x}\text{Ti}_x\text{O}_3$ ($0 \leq x \leq 0.30$) ceramics. The selected compositions were summarized in Table 1.

Table 1. Composition of the mixtures investigated

Mixture	Composition
1	BiFeO ₃
2	Bi _{0.95} Ba _{0.05} Fe _{0.95} Ti _{0.05} O ₃
3	Bi _{0.90} Ba _{0.10} Fe _{0.90} Ti _{0.10} O ₃
4	Bi _{0.85} Ba _{0.15} Fe _{0.85} Ti _{0.15} O ₃
5	Bi _{0.80} Ba _{0.20} Fe _{0.80} Ti _{0.20} O ₃
6	Bi _{0.75} Ba _{0.25} Fe _{0.75} Ti _{0.25} O ₃
7	Bi _{0.70} Ba _{0.30} Fe _{0.70} Ti _{0.30} O ₃

The place of the selected compositions on the BiFeO₃ – BaTiO₃ tie line of the quaternary Bi₂O₃ – BaO – Fe₂O₃ – TiO₂ system is also presented in Fig. 1.

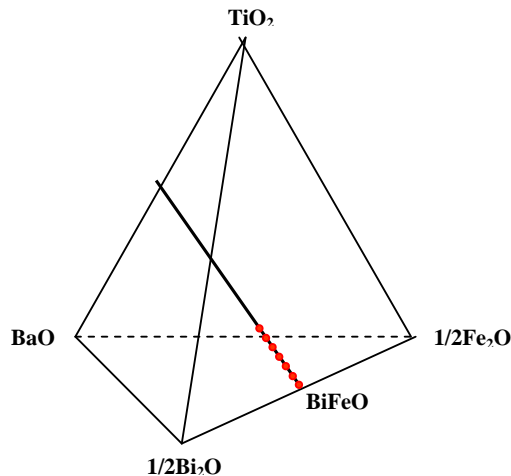


Fig. 1. Place of the selected compositions in the quaternary Bi₂O₃ – BaO – Fe₂O₃ – TiO₂ system.

2. Experiment

Sample preparation

Samples with the mentioned composition were prepared by classical solid state reaction method from high purity oxides and carbonates: Bi₂O₃ (Fluka), Fe₂O₃ (Riedel de Haen), TiO₂ (Merck) and BaCO₃ (Fluka), by a wet homogenization technique in isopropyl alcohol. The mixtures were granulated using a 4 % PVA (polyvinyl alcohol) solution as binder agent, shaped by uniaxial pressing at 160 MPa into pellets of 20 mm diameter and ~ 3 mm thickness. The presintering thermal treatment was carried out in air, at 650°C, with 2 hours plateau. The samples were slowly cooled, then ground, pressed again into pellets of 10 mm diameter and 1- 2 mm thickness and

sintered in air, with a heating rate of 5°C/min, for 1 hour at 700 and 800°C, respectively.

Sample characterization

X-ray diffraction measurements at room temperature, used to investigate the purity of the perovskite phase in the presintered powders, as well as in the sintered pellets were performed with a SHIMADZU XRD 6000 diffractometer using Ni-filtered CuK α radiation ($\lambda = 1.5418 \text{ \AA}$), with a scan step of 0.02° and a counting time of 1 s/step, for 2 θ ranged between 20° and 80°. The microstructure of the ceramics was examined by scanning electron microscopy, using a Hitachi S2600N equipment. The Raman spectra in the range of (100, 1000) cm⁻¹ wavelength at room temperature were recorded in back-scattering geometry by using a RENISHAW RM2000 micro-Raman spectrometer with 785 nm radiation, 2 μm spot diameter and 10 μm field depth. The electrical measurements were performed on parallel-plate capacitor configuration, by applying Pd-Ag electrodes on the polished surfaces of the sintered ceramic disks. The complex impedance in the frequency domain (20 $\div 2 \times 10^6$ Hz at temperatures below 200°C was determined by using an impedance bridge type Agilent E4980A. The magnetic moments were measured in the range of (5 \div 350) K using a superconducting quantum interferometric magnetometer SQUID (Quantum Design) and above the room temperature by using a VSM (Lake Shore 7410). The samples were cooled down to the measurement temperature in the absence of the magnetic field (zero-field cooling ZFC). The field was subsequently applied while heating (field heating FH) for the measurement of the temperature dependence on the magnetic moment.

3. Results and discussions

The room temperature X-ray diffraction patterns obtained for both presintered and sintered samples show single-phase compositions for all the mixtures investigated (Fig. 2 and Fig. 3).

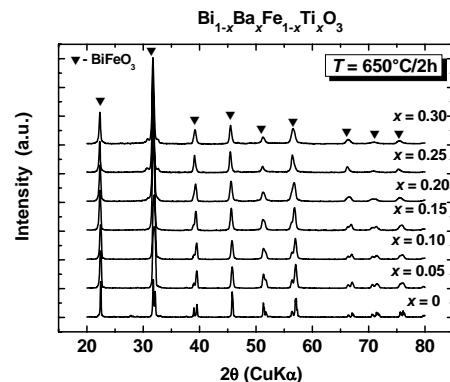


Fig. 2. Room temperature X-ray diffraction patterns of Bi_{1-x}Ba_xFe_{1-x}Ti_xO₃ powders presintered at 650°C for 2 hours.

The unique phase identified was that one corresponding to the rhombohedral BiFeO_3 for the mixture 1, and to the perovskite $\text{Bi}_{1-x}\text{Ba}_x\text{Fe}_{1-x}\text{Ti}_x\text{O}_3$ solid solutions for the mixtures 2 – 7. The gradual change of the rhombohedral structure toward a cubic one with the increase of BaTiO_3 addition is proved by the cancellation of the X-ray diffraction splitting specific to pure BiFeO_3 . The processing procedure involving the first thermal treatment stage (presintering) performed on pressed samples and not on powdered mixtures and thus favouring complete chemical reactions may be responsible for the lack of Bi-rich non-equilibrium secondary phases. Further investigations are required in order to calculate the lattice parameters and to determine the substitution degree at which the rhombohedral unit cell completely changes to a cubic symmetry.

SEM analyses were performed on the surface of the pellets sintered at $800^\circ\text{C}/1\text{h}$. The SEM micrograph of the BiFeO_3 ceramic (sample 1) shows a heterogeneous microstructure with bimodal grain size distribution, consisting from large grains with equivalent average size of $\sim 25\ \mu\text{m}$ and small grains of $3 - 4\ \mu\text{m}$ (Fig. 4). The micrographs of samples 4 and 7 (Fig. 5, 6) show that the BaTiO_3 addition influences drastically the microstructure (Fig. 3).

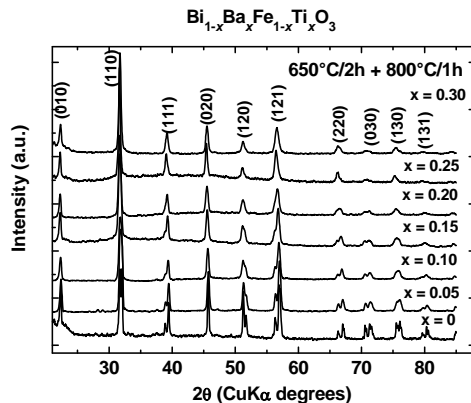


Fig. 3. Room temperature X-ray diffraction patterns of $\text{Bi}_{1-x}\text{Ba}_x\text{Fe}_{1-x}\text{Ti}_x\text{O}_3$ pellets sintered at 800°C for 1 hour.

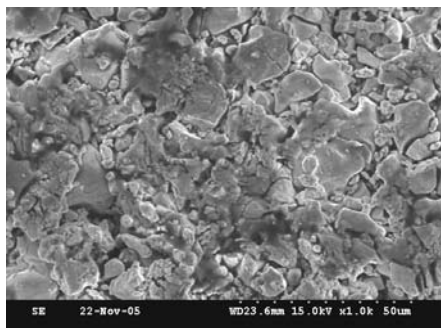


Fig. 4. Surface SEM image of BiFeO_3 sample sintered at $800^\circ\text{C}/1\text{h}$.

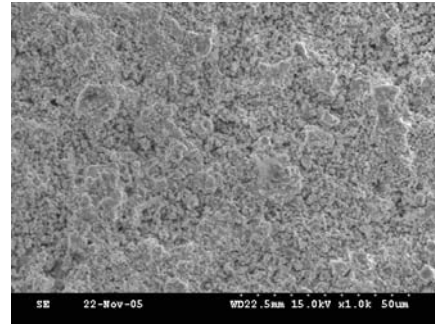


Fig. 5. Surface SEM image of $\text{Bi}_{0.85}\text{Ba}_{0.15}\text{Fe}_{0.85}\text{Ti}_{0.15}\text{O}_3$ sample sintered at $800^\circ\text{C}/1\text{h}$.

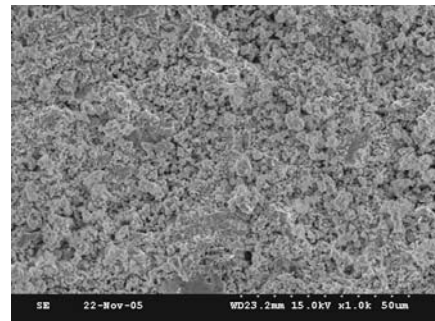


Fig. 6. Surface SEM image of $\text{Bi}_{0.70}\text{Ba}_{0.30}\text{Fe}_{0.70}\text{Ti}_{0.30}\text{O}_3$ sample sintered at $800^\circ\text{C}/1\text{h}$.

One can observe the inhibiting effect of the barium titanate used as additive on the grain growth process and, consequently, a relative homogenous microstructure, with intergranular porosity, and finer (submicron) grains than those ones of similar, non-modified sample was formed, in both cases analyzed here.

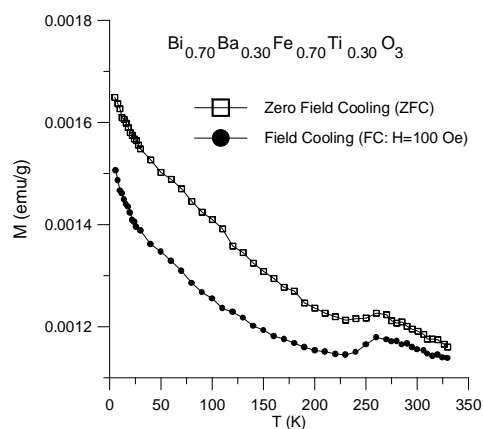


Fig. 7. Temperature-dependence of the magnetic moments at a FC/ZFC sequence of the $\text{Bi}_{0.70}\text{Ba}_{0.30}\text{Fe}_{0.70}\text{Ti}_{0.30}\text{O}_3$ ceramic sample.

The functional properties of some compositions were also determined. Fig. 7 shows the temperature dependence of the magnetic moment at a FC/ZFC sequence for the ceramic sample with composition $\text{Bi}_{0.70}\text{Ba}_{0.30}\text{Fe}_{0.70}\text{Ti}_{0.30}\text{O}_3$. The anomalies detected below 20 K and in the range of (250, 300) K shows the presence of at least two magnetic phase transitions, the first one being from a weak ferromagnetic-to-antiferromagnetic state. The calorimetry data did not reveal any features in the range of temperatures of (100, 375) K and only an anomaly at (375, 475) K not associated to structural changes can be attributed to a transition from antiferro-to-paramagnetic state. It results that most probably the magnetic phase transition around the room temperature is between two types of antiferromagnetic order, due to some kind of rearrangements of the canted spins. Consequently, this composition will be most probably antiferromagnetic at room temperature. In fact, the recorded hysteresis loops at room temperatures shows almost zero remanent magnetisation and as saturation of ~ 1.2 emu/g for a field of $H=20$ kGauss (Fig. 8).

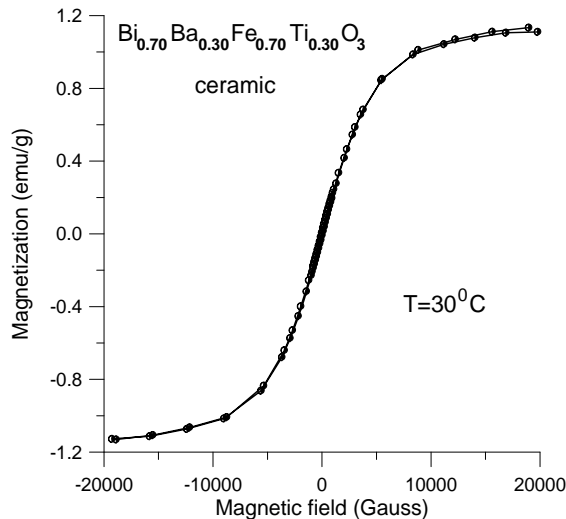


Fig. 8. Magnetic hysteresis loops at the room temperatures obtained for the $\text{Bi}_{0.70}\text{Ba}_{0.30}\text{Fe}_{0.70}\text{Ti}_{0.30}\text{O}_3$ sintered ceramic.

Further accurate experiments above the room temperature are expected to clarify the nature of the magnetic transitions in the ceramic with composition $\text{Bi}_{0.70}\text{Ba}_{0.30}\text{Fe}_{0.70}\text{Ti}_{0.30}\text{O}_3$. In any case, this ceramic presents a kind of magnetic order at room temperature.

The real and imaginary part of the dielectric constant for the $\text{Bi}_{0.70}\text{Ba}_{0.30}\text{Fe}_{0.70}\text{Ti}_{0.30}\text{O}_3$ ceramic at the frequency of 1 kHz (Fig. 9) shows that at room temperature this composition has good dielectric properties, with losses below 3%.

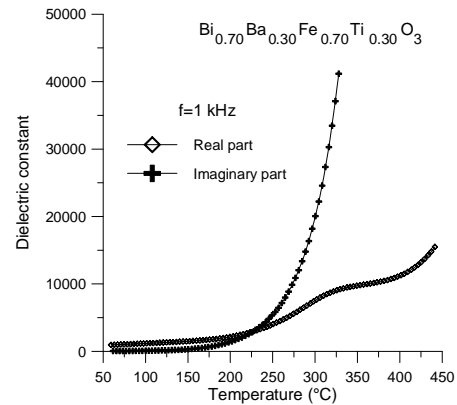


Fig. 9. Temperature-dependence of the real and imaginary part of the dielectric constant for $\text{Bi}_{0.70}\text{Ba}_{0.30}\text{Fe}_{0.70}\text{Ti}_{0.30}\text{O}_3$ ceramic sample.

The losses are still acceptable for such a system by comparing with other literature data [8-10], up to around 220°C when $\tan \delta < 1$. However, by increasing more the temperature above this value, a giant increase of the imaginary part of permittivity with temperature takes place and the material is not dielectric anymore. Looking to the real part of the permittivity, it is possible to locate the ferroelectric-paraelectric anomaly in the range of (250, 375)°C, similar as reported in the ref. [9]. In spite the very high values of the dielectric constant above 10000 and to the diffuse aspect of the phase transition similar as in relaxors, a quantitative description of such a behaviour as performed in [9] is not indicated. The high measured permittivity is not related to good dielectric/ferroelectric character, but is a false value due to some thermally-activated conduction mechanisms. The polar character (intrinsic ferroelectricity) is in any case preserved at room temperature, as demonstrated by the presence of the ferro-paraelectric phase transition at much higher temperatures of (250, 375)°C. It results that this composition is a multiferroic at room temperature, where also the losses are rather small. As mentioned before, the conduction phenomena in BiFeO_3 are still under debate. The solid solutions BiFeO_3 - BaTiO_3 are even more complicated. The role of polaronic and ionic conductivity associated to the formation of oxygen vacancies as compensating defects for the partial reduction certainly contribute to the thermally-activated conductivity. Therefore, this is not the only one possible mechanism. The evolution with temperature of the impedance spectra together with other microstructural investigations on the charged defects will give a more precise answer concerning the origin of the observed impedance components.

An attempt to observe compositional or local crystalline symmetry-induced changes in regions at the grain bulk/boundary for this composition by micro Raman technique at room temperature was done, due to the fact that this technique is more sensitive than the XRD experiment accuracy. In addition, the Raman activity is indicating the polar state of the system (i.e. its ferroelectric property), since no Raman activity is allowed in a cubic

symmetry. Many local Raman spectra were recorded by focusing the laser beam in various locations at the interior of a ceramic grain or at grain boundaries.

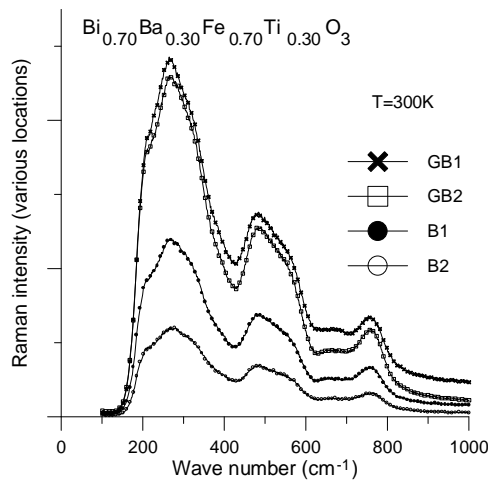


Fig. 10. Raman spectra at room temperature collected at a few locations at the surface of the $\text{Bi}_{0.70}\text{Ba}_{0.30}\text{Fe}_{0.70}\text{Ti}_{0.30}\text{O}_3$ ceramic: (GB1 and GB2: data collected when the laser beam was focused at the grain boundaries, B1 and B2: inside the grain bulk).

Fig. 10 presents such spectra obtained in two ceramic grain boundaries (denoted as GB1 and GB2) and inside two grains (denoted as B1 and B2). A very good reproducibility of the spectra was found in many locations and the same vibration bands, indicating an average good compositional homogeneity, no presence of other phases below the XRD sensitivity or local structural deviations. Only very small changes in the ratio of intensities of some peaks like for example 470 cm^{-1} and 560 cm^{-1} , shifts of the peak position for the 650 cm^{-1} and 760 cm^{-1} bands and mainly the intensity of the 769 cm^{-1} band are evidences of some small local changes inside the material, but these can also be related to small internal stresses or differences in the ceramic grain orientations inherent inside a ceramic material, as well. A careful Raman analysis at various temperatures is expected to give more information on the peaks evolution. At this stage of the present research, it results that the impedance behaviour is not related to segregation of other phase or to local structural deviations from the $R3c$ symmetry.

4. Conclusions

$(1-x)\text{BiFeO}_3 - x\text{BaTiO}_3$ ($0 \leq x \leq 0.30$) ceramics were prepared by the solid state reaction method. After sintering at $800^\circ\text{C}/1\text{h}$ and slow cooling, single phase compositions were obtained for all the mixtures analyzed. The gradual attenuation of the rhombohedral distortion with the increase of BaTiO_3 content was pointed out. The BaTiO_3 admixture acts also as inhibitor for the grain growth process, contributing to the decrease of the average grain size. The composition corresponding to $x = 0.30$ proved to be multiferroic at room temperature, having both antiferromagnetic and ferroelectric order and low losses ($< 3\%$). At high temperatures, thermally-activated processes seriously affect the dielectric properties. Some differences in the Raman spectra indicate some local inhomogeneity of the dielectric/conductive characteristics inside the ceramic body. These changes are not related to the presence of segregated phases at grain boundaries or to changes of the local crystalline symmetry.

Acknowledgements

This work was supported by the Romanian CNCSIS grant CONSMEMF (2006-2008).

References

- [1] I. H. Ismailzade, R. M. Ismailov, A. I. Alekberov, F. M. Salaev, *Phys. Status Solidi A*, **57**, 99 (1980).
- [2] I. H. Ismailzade, R. M. Ismailov, A. I. Alekberov, F. M. Salaev, *Phys. Status Solidi A*, **68**, K81 (1981).
- [3] I. H. Ismailzade, R. M. Ismailov, *Phys. Status Solidi A*, **59** (1980) K191-194.
- [4] P. Fischer, M. Polomska, I. Sosnowska, M. Szymanski, *J. Phys. C: Solid State Phys.*, **13**, 1931 (1980).
- [5] F. Kubel, H. Schmid, *Acta Crystallogr., Sect. B: Struct. Sci.*, **46**, 702 (1990).
- [6] C. Blaauw & F. van der Woude, *J. Phys. C: Solid State Phys.*, **6**, 1422 (1973).
- [7] E. I. Speranskaya, V. M. Skorikov, E. Ya. Rode & V. A. Terekhova, *Bull. Acad. Sci. USSR, Div. Chem. Sci.*, **1965**, 873 (1965).
- [8] M. M. Kumar, A. Srinivas, G. S. Kumar, S. V. Suryanarayana, *J. Phys.: Condens. Matter.*, **11**, 8131 (1999).
- [9] M. M. Kumar, A. Srinivas & S. V. Suryanarayana, *J. Appl. Phys.*, **87**, 855 (2000).
- [10] W. M. Zhu & Z. G. Ye, *Ceram. Int.*, **30**, 1435 (2004).

*Corresponding author: lmtrs@uaic.ro